Fermi National Accelerator Laboratory

FERMILAB-Conf-90/110

SDC at High Luminosity *

Dan Green
Fermi National Accelerator Laboratory
P.O. Box 500
Batavia, Illinois 60510

May 1990

* Presented at the International Conference on Solenoidal Detectors for the SSC, Tsukuba, Japan, April 23-25, 1990.

Operated by Universities Research Association Inc. under contract with the United States Department of Energy

SDC AT HIGH LUMINOSITY

by

Dan Green
Fermi National Accelerator Laboratory

1.0 Introduction

Why is it prudent to plan for a luminosity (L) of $> 10^{34}/(cm^2 sec)$ from the beginning? First, the SSC is easily capable of attaining high luminosity. In comparison, for $\bar{p}p$ machines such as the Tevatron, increases in L are difficult. Second, after early runs at design luminosity, the only simple upgrade to a general purpose detector is an increase in luminosity. Third, and most important, the only known model independent physics goal of SSC is in the electroweak sector; the ZZ scattering amplitude reaches the unitarity bound(1) for $\sqrt{\hat{s}} \simeq 3$ TeV. In order to reach this mass range, and assure that some new physics is found, high luminosity running is needed. Since high luminosity running is desirable and easily attainable, it is inevitable. Therefore, one should build the "hooks" for upgrades to high L into the SDC from the beginning. The experience of CDF is that if this is not done, upgrades can be painful. Specifically, if possible, SDC should make sure that the chosen technologies allow high L operation. The time to plan for the whole useful lifetime of SDC is from the beginning.

2.0 Physics Reach

A generic partonic cross section is(2):

$$d\sigma/dM \sim \alpha_{EFF}^2(1 - \ - M/\sqrt{s})^{\beta}/M^3$$
$$<x> \simeq M/\sqrt{s}, \ \beta \sim 12. \qquad (1)$$

The physics reach for a 10 fold increase in L depends on the process. For Higgs searches, $\alpha_{EFF} \simeq \alpha_w$ and the weakness of the coupling means that search limits at design luminosity are at $M \lesssim 0.8$ TeV or $<x> \lesssim 0.02$. The source distributions are then, $(1 - <x>)^{\beta} \sim 1$ so that a 10 fold increase in L leads to a $(10)^{1/3} \simeq 2$ fold increase in mass reach.

For dijets, with strong coupling $\alpha_{EFF} \sim \alpha_s$, one can reach $M_{JJ} \simeq 10$ TeV ($<x> \sim 0.25$) at design luminosity. A 10 fold increase in L only leads to a factor 1.3 increase in M_{JJ}, since one is now limited by the source functions. Thus, the two gauge boson search gains most with L

since one is limited by statistics, but is at low <x>. By comparison, dijet physics is likely to be best done at or below design luminosity.

Where in phase space is the multi-TeV physics scale? The central (wide angle) region is the discovery region. For example, a 2 TeV mass object has a kinematic limit of $y_{MAX} \sim 3.0$

$$y_{MAX} = \ln (1/\langle x \rangle). \tag{2}$$

Clearly, allowing two units of rapidity to fall off the "plateau," multi-TeV masses populate only the central region. Figure 1 shows that there is little loss in cross section due to sources even with soft gluons if $M \lesssim 4$ TeV, while for $M \gtrsim 2$ TeV only the central (barrel) ± 1.0 unit of y is populated. Therefore, only the central barrel region needs to function at high luminosities since the forward region is depopulated for these high mass objects.

3.0 Radiation Dose

A crucial issue for high luminosity detector performance is obviously the radiation dose. The maximum dose comes in the electromagnetic calorimeter, since the energy deposition is most concentrated there. The energy deposited by one m.i.p. crossing a plane of material of density ρ, volume V is roughly:

$$\text{e.m.i.p.} = (\sigma_I \, LT) \; (1/\sigma_I \; d\sigma/dy) \; (1/2\pi R_\perp^2)\Delta E \rho V, \tag{3}$$

where σ_I = inelastic cross section, L = luminosity, T = dose time, $R_\perp$ = transverse distance, and $\Delta E \simeq 1.8$ MeV/(gm/cm^2). Approximating $P_\perp \simeq \langle P_\perp \rangle \simeq 0.5$ GeV, then $P \simeq \langle P_\perp \rangle/\sin\theta$. The number of shower m.i.p.s. at shower maximum in the EM detector is $\equiv n_e^{MAX} P = n_e^{MAX} \langle P_\perp \rangle/\sin\theta$. The maximum energy deposit, and dose are:

$$\begin{aligned} E_{MAX} &= (\text{e.m.i.p.}) \; n_e^{MAX} \langle P_\perp \rangle/\sin\theta \\ \text{dose} &= (E_{MAX})/(V\rho). \end{aligned} \tag{4}$$

Numerically, for $\sigma_I = 100$ mb, $L = 10^{34}/(\text{cm}^2\text{sec})$, $T = 10^7$sec/yr, $(1/\sigma_I \; d\sigma/dy) = 3\pi^0$/unit of rapidity, $n_e^{MAX} = 10 \; e$/(GeV incident),[3] the dose is $\simeq 21$ krad for $\theta = 90°$, $R_\perp = 2.0$m, and 3.4 Mrad for $y = 3$, $z = 5.0$m, $R_\perp = 0.5$m for plastic scintillator. These limits are almost attainable, in that samples of scintillator (green) exposed to 1 Mrad suffer only modest changes in light output.[4] The goal of preserving the operation of the central barrel over the roughly 10 year life of SDC, operated at high luminosity, seems almost possible. In what follows one assumes that the "discovery" region is not impaired for calorimetry. However, the $1/(R_\perp^2 \sin\theta)$ behavior of Eq. 4 means that $y \gtrsim 3$ is problematic for calorimetry. Hence the missing E_T measurements will be compromised.

Tracking will exist at lower $R_\perp$, but will not suffer the increase in m.i.p.s. due to an electromagnetic shower. Ignoring neutron albedo leaking back into the tracking detectors,[5] one finds that at 90°; $R_\perp = 1.5$m, dose ~ 21 krad $(2.0/1.5)^2(2)/5$ ~ 15 krad/year. It seems plausible that radiation hard tracking could be made to work in this radiation field. Clearly, from Eq. 3, the dose goes as $1/R_\perp^2$. By comparison, the momentum resolution is proportional to $1/R_\perp^2$ in the barrel. Much optimization of dose vs. resolution clearly needs to be done. The stable operation of both detectors and readout electronics becomes problematic for detector radii much less than 1.5m.

As a simple example of a system at large radii consider a set of scintillating fibers 1mm x 1mm x 4m in two superlayers (xx'uv + xx'uv). Such a minimal system has 150,000 channels of readout. In the case of fibers, there is neither gain (heat) nor electronics (heat and radiation damage) within the solenoid volume; all power is dissipated outside the calorimeter volume - which also acts as a radiation shield. This layout also offers a potential commonality of tracking and calorimeter readout-pipeline and triggering. As noted above,[5] the "sea" of albedo neutrons has not been discussed. Clearly, the response of scintillating fibers, or any other tracking detector, immersed in this "sea" is a crucial problem to be given detailed study.

4.0 Quark, Lepton, and Boson Identification

Increasingly, one can think of the task of general purpose collider detectors to be that of detecting partons. The gauge bosons to identify are γ, $W^\pm$, Z^0, and g. The fermions are leptons (e, μ, τ, and ν) and quarks (u, d, s, c, b, and t). The main question is if, indeed, the possible necessity of operating tracking detectors only at $R_\perp \gtrsim 1.5$m has severly compromised the physics. Specifically, have we lost the 2 gauge boson physics which we raised the luminosity in order to gain?[6]

For tracking, assume two superlayers at $R_\perp = 1.5$m to 2.0m. The radiation dose seems tolerable at $L = 10^{34}/(\text{cm}^2\text{sec})$. For $\Delta y = 2$ length elements, there are roughly 480 charged tracks. Assuming 1mm diameter elements, the occupation level is only 2.5% (1 track every 5 cm of azimuthal distance). Clearly pattern recognition appears possible at least in principle. Given two layers separated by 50 cm, one can resolve angles of ~ 1 Mrad. In a 2T field, a 1 TeV track bends 1 Mrad in 1.5m, or $(dP_\perp/P_\perp^2)$ ~ $(1\ \text{TeV})^{-1}$. This value for the resolution assumes that the vertex is known from accelerator scans. The tracking "stubs" then give a redundant measurement of energy to compare to the electromagnetic calorimeter. $dE/E \simeq 0.15/\sqrt{E} \oplus 0.01$.

At this point, detailed studies of particle identification at high L have not been made. However, some obvious and superficial comments can still be made. To lowest order, high $P_\perp$ jets (in the multi-TeV range) are not seriously altered by high luminosity: u, d, s, c, b, t, g are still usable. Since γ and e (and hence W, Z) are detected primarily by calorimetric means, they too will be largely uneffected. Since calorimetry will be difficult for $y \geq 3$, missing $E_\perp$, or ν tagging will be compromised. Secondary vertices (c, b, t) are probably impossible at high L. Conversely, these processes occur inclusively at high rate and will be well studied at low L. Finally, muon momentum measurement, but not identification, is compromised by the loss of momentum resolution. The proposed SDC muon system has some "stand alone" capability with room for added detector planes as part of a high L upgrade. The mass resolution for $Z \to \mu\mu$ is degraded, but if the S/N is acceptable a constrained fit to $M_{\mu\mu} \equiv M_Z$ can be made.

5.0 Z, ZZ Resolution at High L

A major physics emphasis of SDC is on 2 gauge boson scattering up to the unitarity limit at $\sqrt{s} \sim 3$ TeV. A one year run at design luminosity will only yield a handful of events of the "gold plated" variety, $H \to ZZ \to 4l$, $l = e, \mu$ for Higgs masses above 600 GeV. It is primarily for this reason that high luminosity running is considered. What compromises are made in detector performance?

Let us begin with the Z natural width, $\Gamma_Z/M_Z \sim \alpha_w$, $\alpha_w \equiv \alpha/\sin^2\theta_w \sim 1/30$. This width sets a natural scale for detector resolutions.

$$\begin{aligned} \Gamma_Z/M_Z &\sim \alpha_w \\ dM_Z/M_Z &= 1/\sqrt{2}(dP_l/P_l). \end{aligned} \tag{5}$$

The comparison is shown in Fig. 2. Clearly, in the e^+e^- final state calorimetry supplies a resolution dM_Z comparable to $\Gamma_Z/2$. In contrast, the tracking has $dM_Z > \Gamma_Z/2$ for all rapidity of interest, as does the toroids. Therefore, signal/noise is degraded. However, with isolation cuts, for example, to reject $t\bar{t}$ background, the S/N for dimuons appears to be acceptable.[7] That being true, one can impose the constraint $M_{\mu^+\mu^-} \equiv M_Z$ and improve the errors on the muon track parameters. In Fig. 2, tracking with $dP_\perp/P_\perp^2 = (1\ \text{TeV})^{-1}$, calorimetry with $dE/E = 0.15/\sqrt{E} \oplus 0.01$, and toroids with $dP_\perp/P_\perp = 0.2$ was assumed.

What about $H \to ZZ$? The scale for the detector resolution is again set by the natural width;

$$\Gamma_H/M_H \sim \alpha w(M_H/M_w)^2$$
$$\Gamma_H \sim 0.5 \text{ TeV } (M_H/\text{TeV})^3 \quad (6)$$
$$dM_H/M_H = 1/2\sqrt{2}\ (dP_l/P_l).$$

The relevant curves are shown in Fig. 3. A constrained fit was assumed for tracking and toroids, but not for calorimetry, since $dM_Z \lesssim \Gamma_Z/2$ in this latter case. It appears that, in the heavy Higgs regime where one wants high L, resolution on the physics (Γ_H) is not compromised for $M_H \gtrsim 0.4$ TeV. Thus, the main goal of high L running is preserved. However, it must be noted that calorimetry and toroids (steel) have a resolution improving with or independent of y, while tracking resolution deteriorates as P ~ cosh y. Thus, at y = 3 the tracking resolution will be perhaps 10 times worse, and the muon system will need to rely on external toroids (perhaps air core). A detailed cost/benefit study needs to be made since the region y = 3 is precisely that region largely depopulated by high mass states (see Fig. 1).

6.0 Pileup Effects

6.1 Minbias:

A serious potential difficulty for high luminosity running is caused by the overlap of ~20 minbias events per bunch crossing. Assuming $\langle P_\perp \rangle \sim 0.6$ GeV and 6 tracks per unit of rapidity, 20 events yield 72 GeV of $P_\perp$ in $|y|<3$ per minimum resolving time of one bunch. Obviously, a global E_T trigger needs a rather higher threshold at higher L.

What about towers? For granularity of $\Delta y \sim 0.05$, $\Delta\phi \sim 0.05$ (10 x 10cm @ 90°, $R_\perp$ = 2.0m), there is only 30 MeV of $P_\perp$/tower in minbias overlap. However, a typical jet of interest has a size at least $R_{cone} \equiv \sqrt{\Delta y^2 + \Delta\phi^2} \sim 0.2$. This means 16 towers in a cluster trigger or ~ 0.5 GeV of $P_\perp$ in minbias. With discovery level at $P_\perp \sim M_{JJ}/2 \sim 5$ TeV (see Section 2.0), the fluctuations in the minbias background cause little problem. High L raises the "underlying event" by 10x in $P_\perp$ scale, but that scale is still very low w.r.t. the SSC discovery scale of multi TeV.

What about triggering on jets? The minbias events have a cross-section which goes as $d\sigma/dP_\perp^2 \sim \exp(-bP_\perp)$, while jets have a power law, hard scattering spectrum, $d\sigma/dP_\perp^2 \sim 1/P_\perp{}^4$. Therefore, the hard scattering physics will always prevail over the soft minbias triggers at suficiently high $P_\perp$. To set the scale, $\langle P_\perp \rangle \sim 2/b \sim 0.6$ GeV per minbias track. The high luminosity overlap level is ~ 0.5 GeV/cluster (1/16 track per tower). Thus, one might apply a threshold cut of 1 GeV per cluster in order for a cluster to add to the jet $P_\perp$ sum. This threshold, on average, subtracts out the underlying pileup of minbias events. The conclusion of an early Snowmass study[8] was that one could simply raise the jet-trigger threshold by a few GeV at high luminosity.

6.2 W → JJ Mass Resolution:

If possible, one wants to preserve the dijet mass resolution at high luminosity. A benchmark for detector performance is $W^- \to \bar{u}d$. Given that the quark fragments uniformly in y, the major problem is in confusing slow fragments of the quarks with the underlying (overlapped) minbias events. The scale is set by the momentum at which that confusion exists;

$$\begin{aligned} dM_{\bar{u}d} &\sim P_{Slow} \\ [M^2_{\bar{u}d} &\sim 2\Sigma_{F,S}\, P_{Slow}\, P_{Fast}\, (1-\cos\theta_{FS})]. \end{aligned} \tag{7}$$

The slow fragments make a large contribution to the dijet mass since they contribute to $M_{\bar{u}d}$ multiplied by fast fragments, and θ_{FS} is large (since at fixed $P_\perp$ fragmentation, the slow fragments make large angles w.r.t. the quark direction). Thus, high L, which raises P_{Slow}, could make a major impact on dijet spectroscopy. A study of this problem has recently been made.[9] The idea was to study the resolution $dM_{\bar{u}d}$ as a function of calorimeter segmentation Δy, $\Delta\phi$ for various levels of pileup. In Fig. 4 is shown dM_W for 1 and 10 overlapped minbias events as a function of $\Delta y = \Delta\phi$. Clearly segmentation, $\Delta y = \Delta\phi \lesssim 0.05$ is preferable. Just as clearly, the jet algorithim confusion level (P_{Slow}) is greater than the intrinsic width $\simeq \Gamma_W/2 \sim 1.2$ GeV by a large factor.

The overlap of 10 events is not a factor 10 worse in dM_W, because (as in jet triggers, section 6.1) a $P_\perp$ threshold is placed on the cluster before it goes into the M_W calculation. This cut worsens dM_W by cutting out real quark fragments, but protects against pileup. More study is needed to optimize this procedure. At present, the tentative conclusion is that high L does not dramatically worsen the W mass resolution.

6.3 Z Pairs and Pileup

Does pileup hurt the Higgs search? In order to make a cursory examination, one notes that, as shown in Fig. 5, σ (ZZ) ~ 30 pb and $d\sigma/dM_{zz} \sim 1/M^3_{zz}$. A possible background comes from accidental Z overlaps from different events. Since $\sigma(Z) \sim 100$ nb, the overlap ZZ background at $L = 10^{34}/(\text{cm}^2\text{sec})$, if the live time is 50 nsec, is;

$$\sigma_{EFF}(ZZ) = \sigma(Z)\ [\sigma(Z)\ \mathcal{L}\Delta t]{=}5\ \text{pb}. \tag{8}$$

which is comparable to σ (ZZ).

Clearly, the scale of $P_{\perp Z}$ for single Z production is O (M_Z), while that for continuum ZZ production is O (M_{ZZ}). The overlap ZZ mass spectrum is, however, harder than the continuum spectrum.

$$\begin{aligned} M_{ZZ}^2 &\sim 2\ M_Z^2[1 + \cosh(\Delta y)] \\ \Delta y &= |y_{z1}\text{-}y_{z2}| \\ d\sigma/dM_{ZZ} &\simeq d\sigma/d(\Delta y)\ [d(\Delta y)/dM_{ZZ}] \sim 1/M_{ZZ}. \end{aligned} \tag{9}$$

The overlap spectrum (from ISAJET) is shown in Fig. 6a. For 1000 (5 pb) overlaps there are 150 events with $M_{ZZ} > 1$ TeV, which is indicative of the long $1/M_{ZZ}$ tail. For $M_{ZZ} = 1$ TeV, Eq. 9 yields $\Delta y = 4$, which is within the barrel region ($|y| < 2$). Assuming $1/M^3$ and $1/M$ behavior respectively, one has $\sigma(ZZ)/\sigma_{EFF}$ (ZZ) ~ 0.24 at M_{ZZ} ~ 1 TeV.

Even so overlap ZZ events are not a problem if the $P_\perp$ spectrum of the Z is well understood. Since $P_{\perp Z}$ is limited, $\langle P_{\perp Z}\rangle$ ~ 26 GeV in ISAJET for overlap ZZ, the overlap events look like very asymmetric decays. Real H → ZZ decays have $P_{\perp Z} \sim M_H/2$ for symmetric ($\cos\theta^* = 0$) decays. In Fig. 6b is plotted the c.m. decay angle, $\cos\theta^*$, for all overlap events treated as H → ZZ decays. Clearly a modest cut of $|\cos\theta^*| < 0.75$ removes almost all overlap events while preserving the majority of the real H → ZZ decays.

7.0 Summary

High luminosity appears to be feasible from an accelerator viewpoint, and desirable in that the electroweak mass reach doubles. Hence, it is probably inevitable and SDC should plan for high $\mathcal{L}$ operation from its inception. Upgrades should be provided for ab initio.

At the mass scales of interest, the central barrel region is populated, while the end caps are not. The radiation dose is such that forward calorimetry is difficult. In the barrel region tracking seems feasible in the outer 50cm directly proceeding the solenoid coil. This tracking lever arm can yield "stubs" which aid electron identification, muon momentum measurements, and give energy measurements at reduced (w.r.t. design luminosity) resolution.

Calorimetry in the barrel is not at radiation risk, although the loss of high y means that the neutrino trigger is compromised. Thus e, μ,and jets will continue to be detectable, although muons will have reduced momentum resolution of $dP_\perp \sim P_\perp^2/(1\text{TeV})$, $dP_\perp \sim 0.2\ P_\perp$.

The loss of y range and μ resolution does not hurt $ZZ \rightarrow 4l$ physics for ZZ masses $\gtrsim 0.4$ TeV. The lower mass scales will be well studied at the design luminosity of the SSC in any case.

The overlap of minbias events does not appear to severely compromise either the jet trigger or the jet $P_\perp$ measurements. Dijet masses appear not to be ruined by pileup, but more realistic studies need to be made. Overlap ZZ events are controlled, if the $P_{\perp Z}$ distribution is limited.

In summary, quite to the authors surprise, high luminosity running looks plausible. Clearly, this is an extremely tentative conclusion and much more detailed studies are required.

References

[1] M. Chanowitz, Ann. Rev. of Nuc. and Part. Sci. 38 323, (1988).

[2] D. Green, $\bar{p}p$ Collider Physics, Fermilab-Conf-89/70.

[3] S. Iwata, DPNU-3-79.

[4] F. Takasaki, High Energy Physics in the 1990's, Snowmass 88.

[5] D.E. Groom, SSC-SR-1033.

[6] T. Skesson et al., The Feasibility of Experiments at High Luminosity at the LHC, CERN 88-02.

[7] L. Nodulman et al., $\bar{t}t$ backgrounds for $H \to \mu^+\mu^-\mu^+\mu^-$ at the SSC, SSC Lab Preprint.

[8] H. Gordon et al., Proceedings of the 1982 DPF Summer Study, Snowmass 82.

[9] A. Bay et al., High Energy Physics in the 1990's, Snowmass 88.

Figure Captions

1.a. Source factor for soft gluons (β=12) as a function of mass.

1.b. Plateau half width as a function of mass for $\sqrt{s}$ = 40 TeV.

2. Reconstructed width of Z bosons as a function of rapidity using calorimetry, (e^+e^- solid curve) tracking ($\ell^+\ell^-$ dashed curve) and muon steel toroids ($\mu^+\mu^-$ dot-dashed curved). Natural width scale is cross hatched.

3. Reconstructed width of Higgs bosons as a function of Higgs mass for y_H = 0 using calorimetry (solid curve), tracking (dashed curve) and steel toroids (dot-dashed curve). Natural width scale is cross hatched.

4. W mass resolution for W → JJ as a function of segmentation for 1 and 10 overlap minbias events.

5.a. ZZ continuum cross section vs. $\sqrt{s}$.

5.b. $d\sigma/dM_{zz}$ for longitudinal and transverse polarizations of ZZ bosons.

6.a. ZZ overlap mass distribution for "accidentals."

6.b. ZZ decay angle, $\cos\theta^*$, assuming H → ZZ.

Figures 1.a. and 1.b.

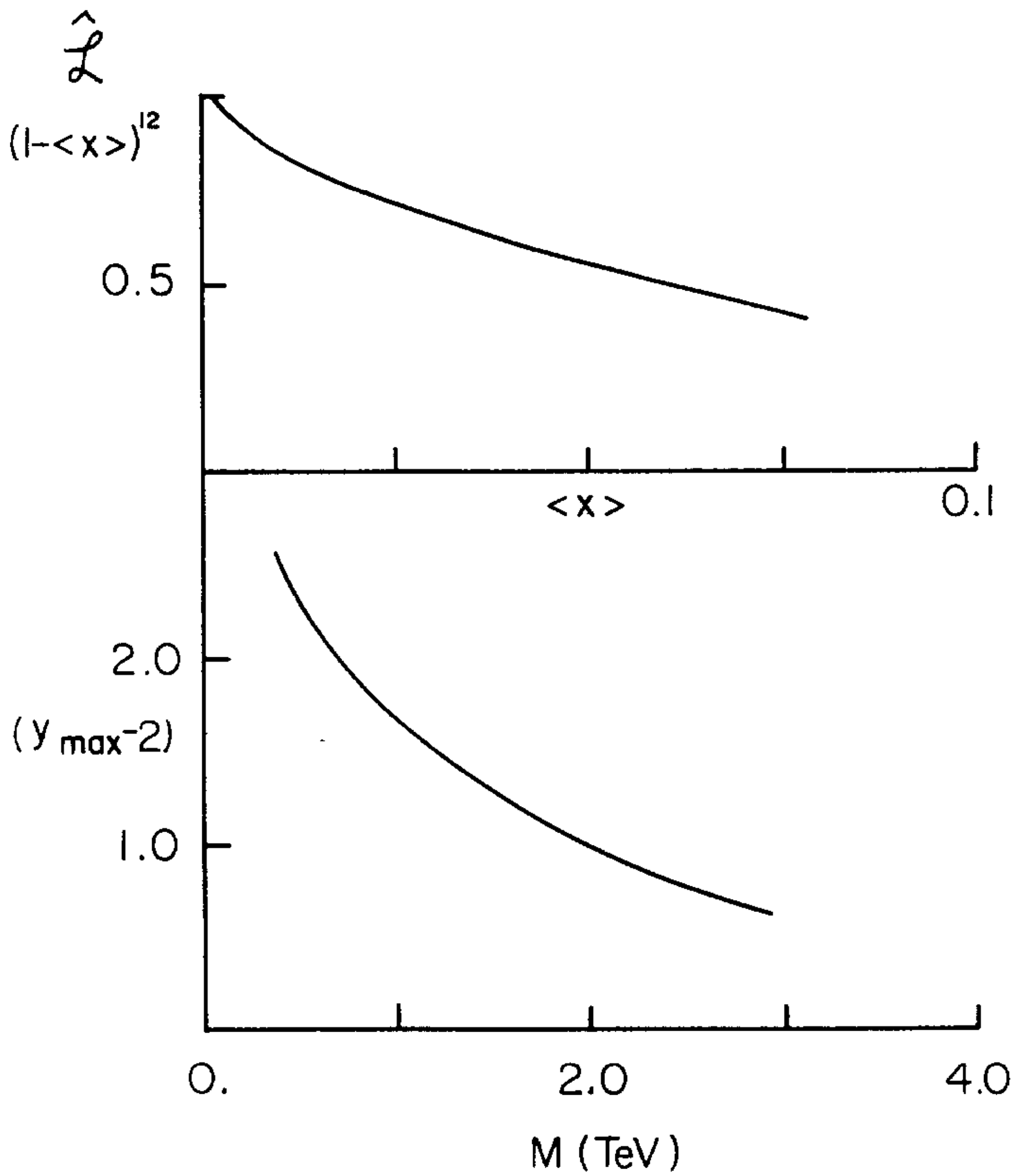

Figure 2.

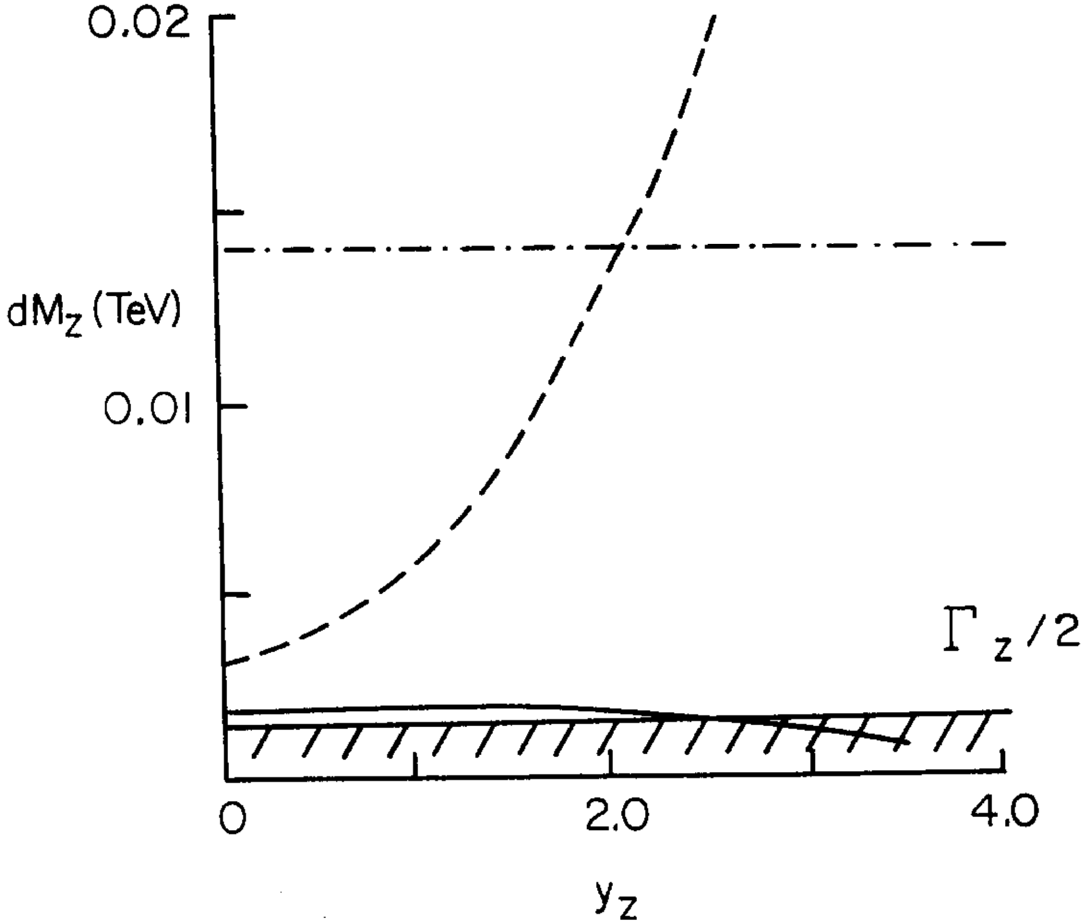

(2)

Figure 3.

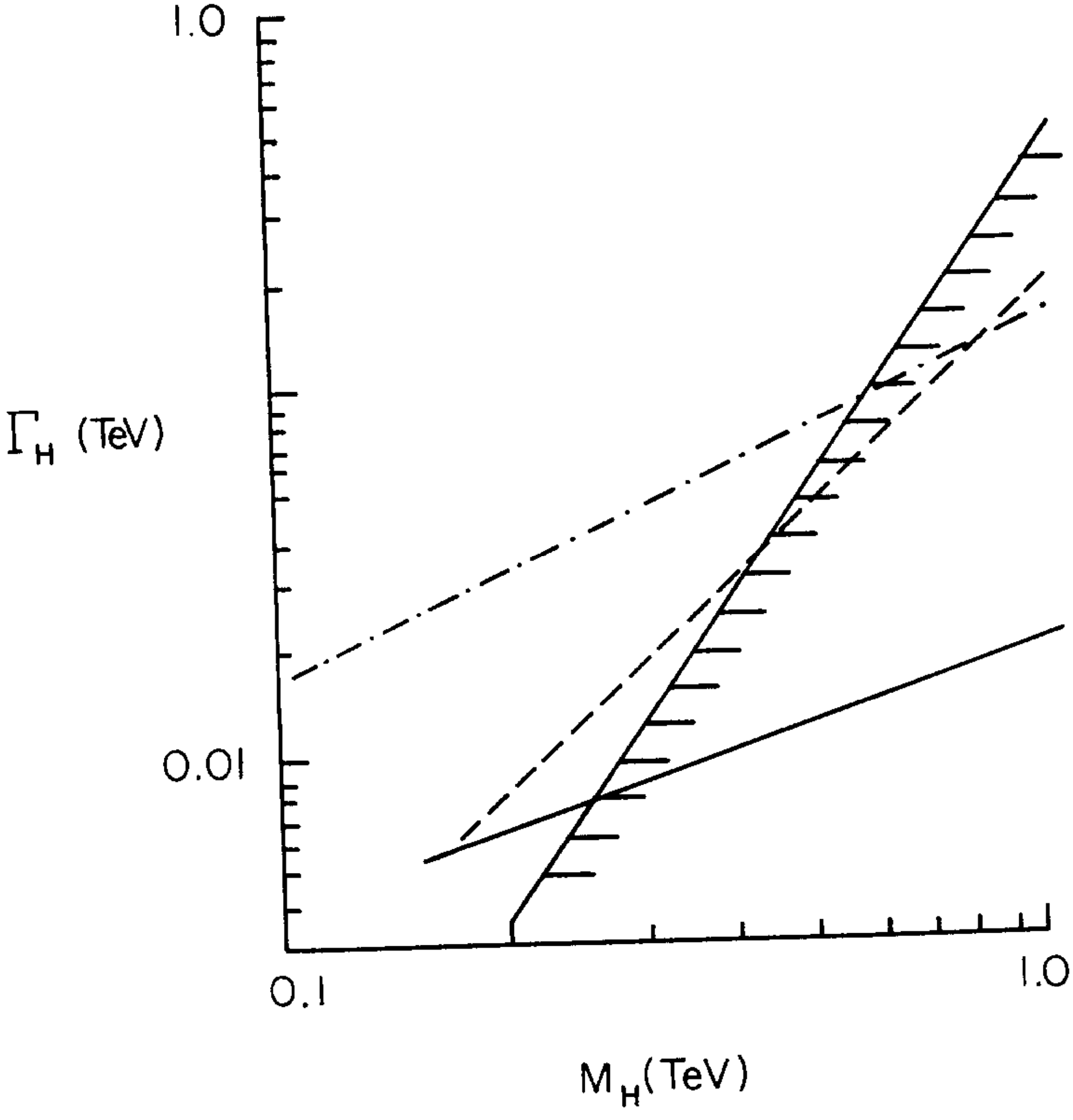

Figure 4.

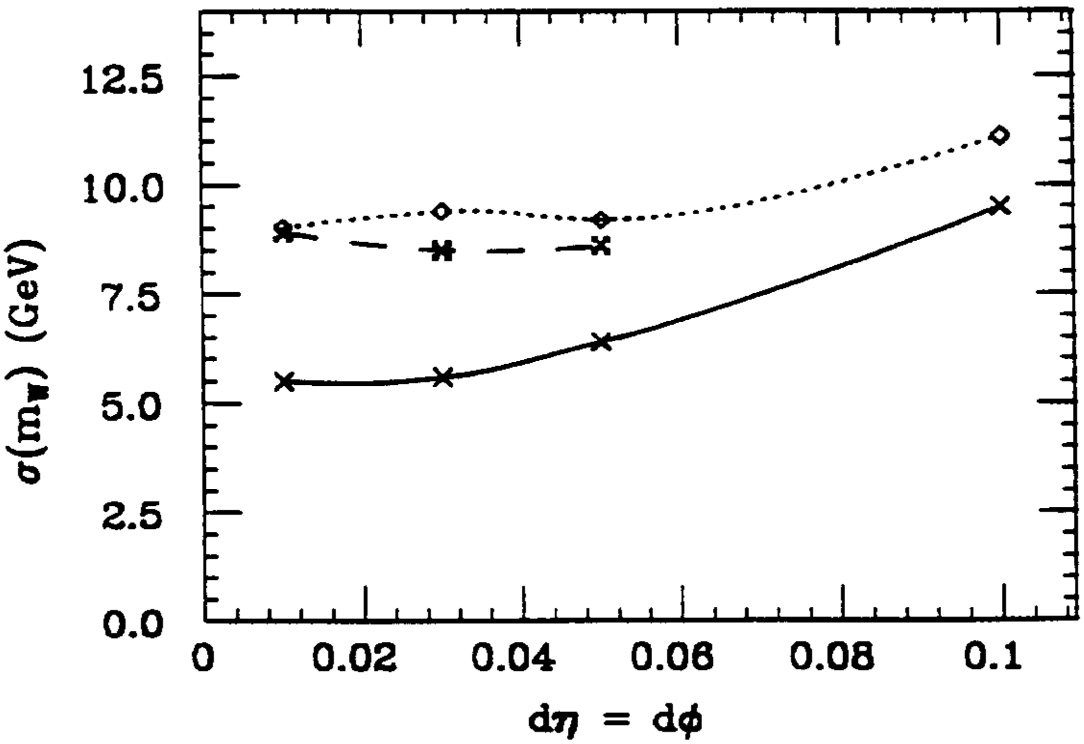

Figure 5.a.

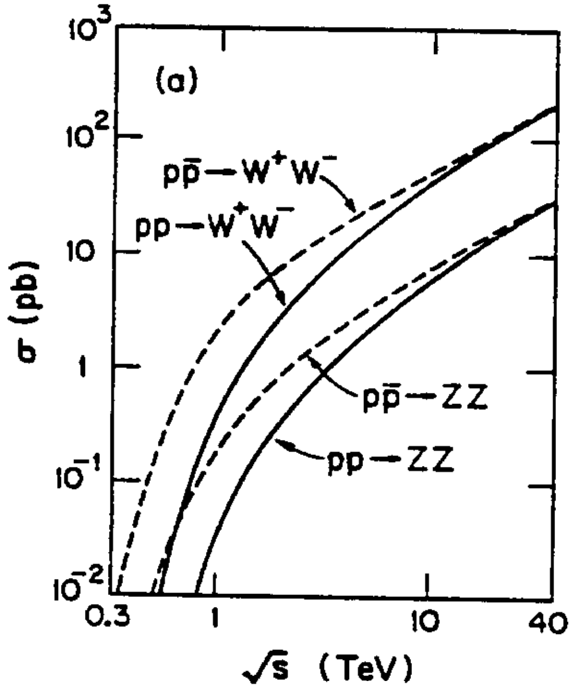

Figure 5.b.

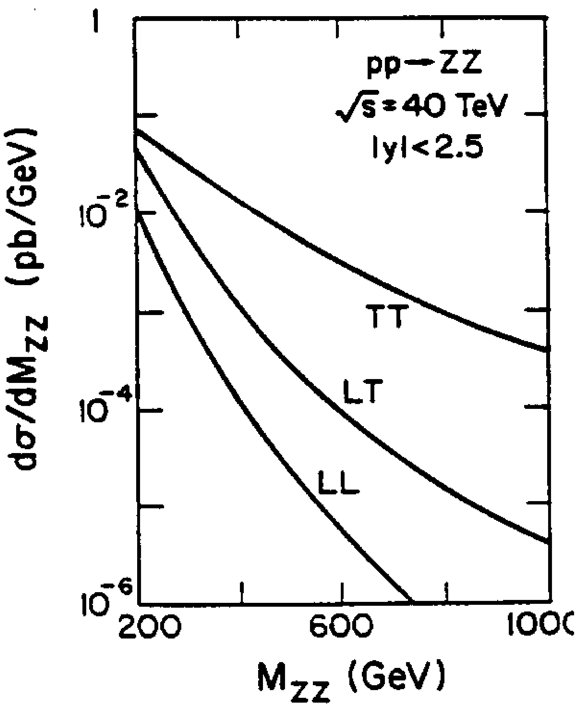

Figure 6.a.

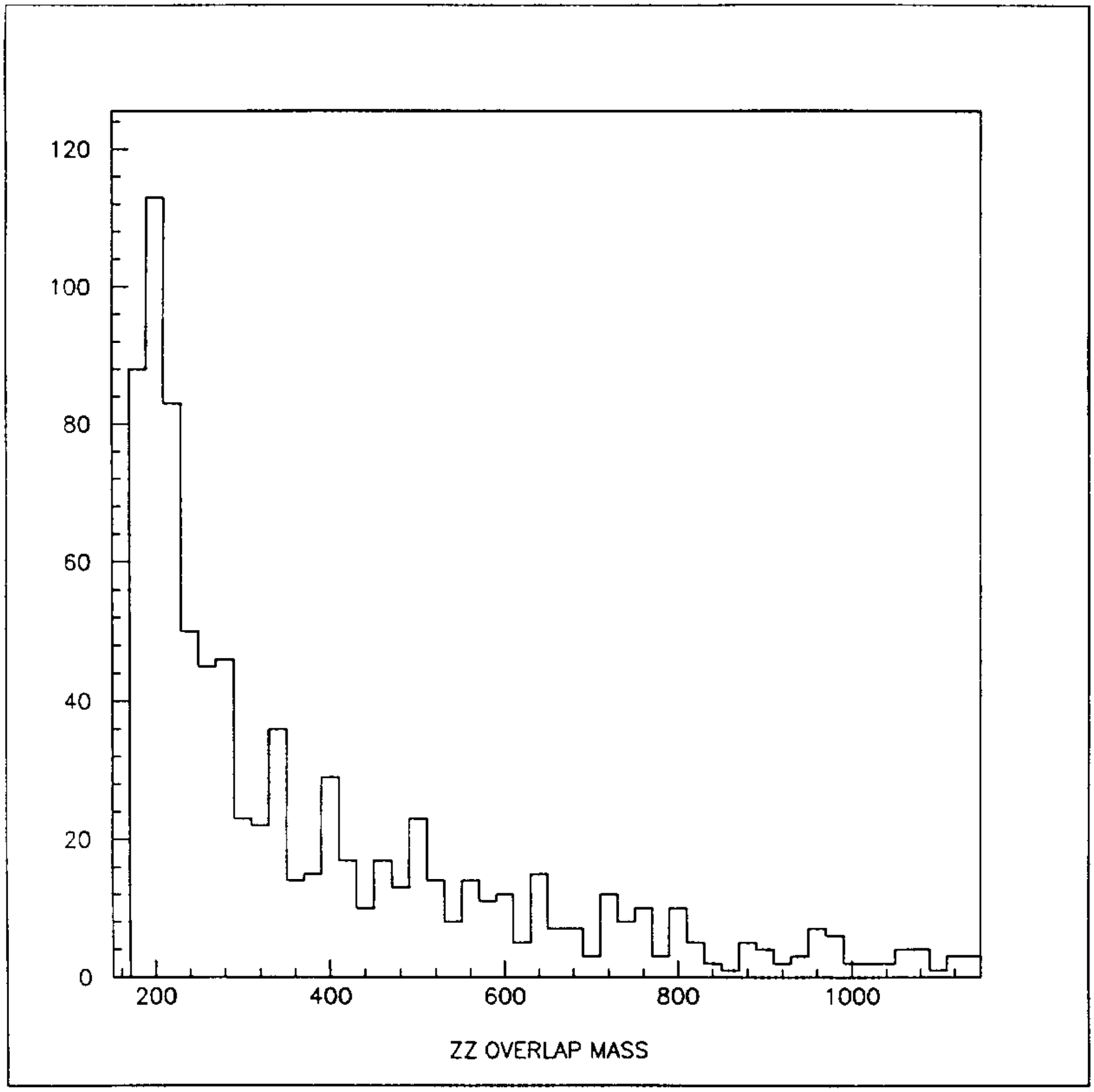

Figure 6.b.

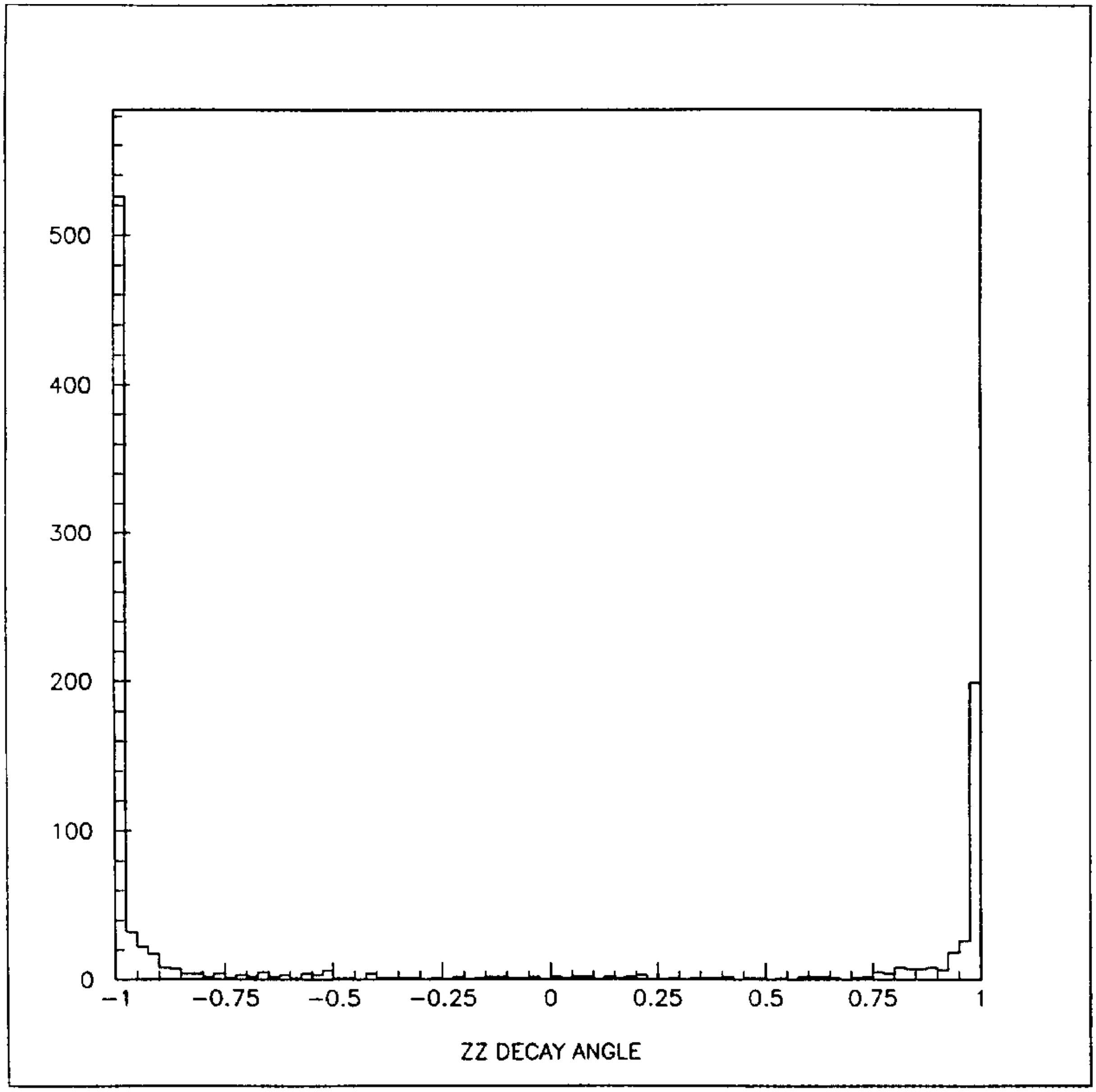

(6 b.